Supplementary Information

Solar-light-driven non-bias photoelectrolysis for bleach production from sea water and O_2 from the air

Corresponding authors

Dr. Shoji IGUCHI and Dr. Kazuhiro SAYAMA

List of the authors

Shoji IGUCHI, Hiroyuki TATENO, Soichi TAKASUGI, Yugo MISEKI, and Kazuhiro SAYAMA

Affiliation and full postal address

Advanced Functional Materials Team, Research Center for Photovoltaics (RCPV), National Institute of Advanced Industrial Science and Technology (AIST), Central 5, 1-1-1 Higashi, Tsukuba, Ibaraki, 305-8565 Japan.

Tel: +81−29−861−4760, Fax: +81−29−861−4760

Table S1 List of chemical contents contained in the artificial sea water MARINE ART SF-1 purchased from Osaka Yakken. Co. Ltd., Japan.

Chemical	Formula	Concentration / mg L^{-1}
Sodium chloride	NaCl	22100
Magnesium chloride	$MgCl_2 \cdot 6H_2O$	9900
Sodium sulfate	Na_2SO_4	3900
Calcium chloride	$CaCl_2 \cdot 2H_2O$	1500
Potassium chloride	KCl	610
Sodium bicarbonate	$NaHCO_3$	190
Potassium bromide	KBr	96
Borax	$Na_2B_4O_7 \cdot 10H_2O$	78
Strontium chloride	$SrCl_2$	13
Sodium fluoride	NaF	3

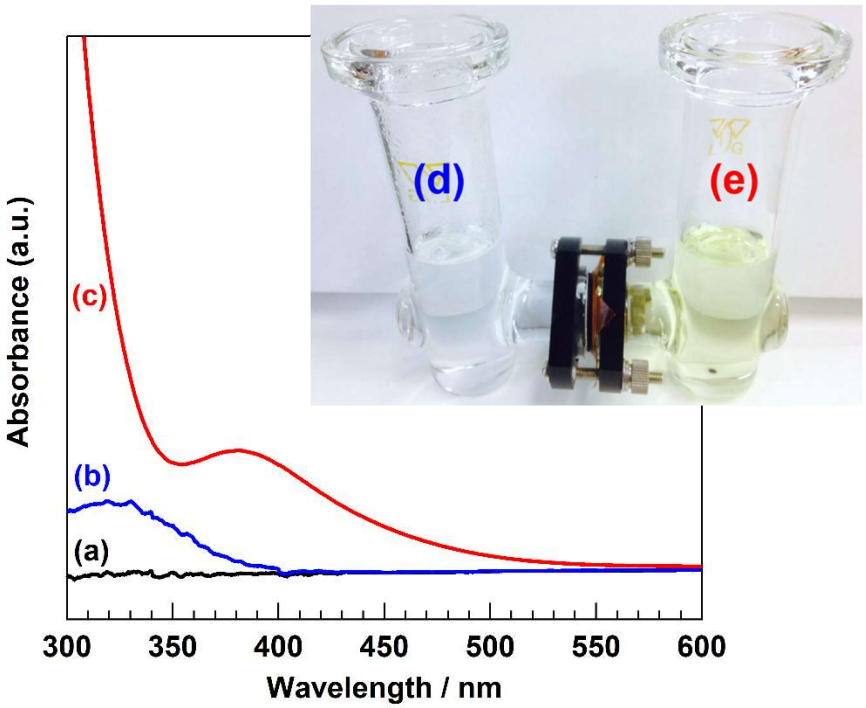

Figure S1 Absorption spectra of (a) NaCl, (b) NaCl + HClO, and (c) NaCl + NaBr + HClO + HBrO, and color comparing of them (d) NaCl + HClO and (e) NaCl + NaBr + HClO + HBrO

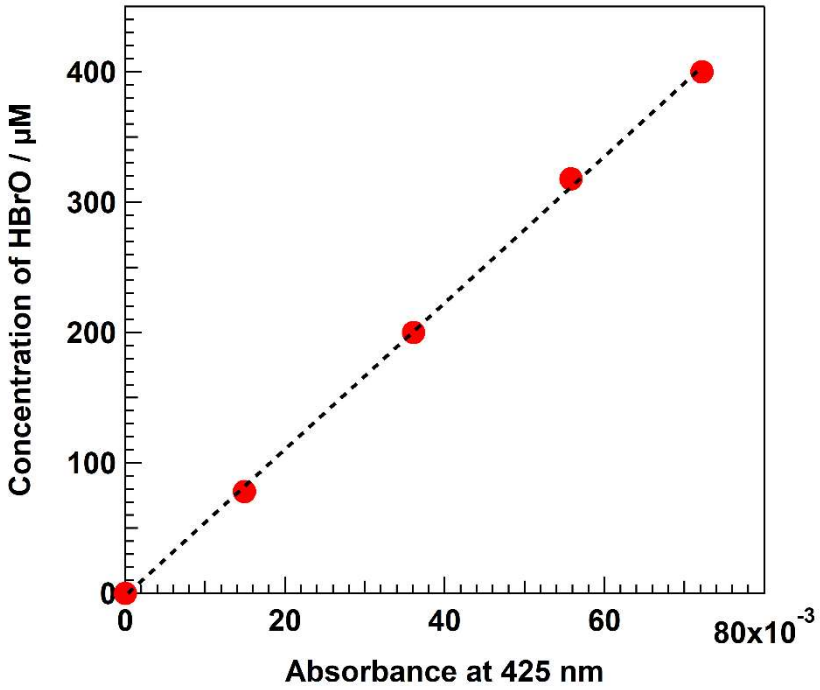

Figure S2 Calibration curve for the determination of HBrO concentration containing in NaCl, NaBr, HClO, and HBrO mixed aqueous solution. Absorption coefficient was clearly influenced by the concentration of Br^-.

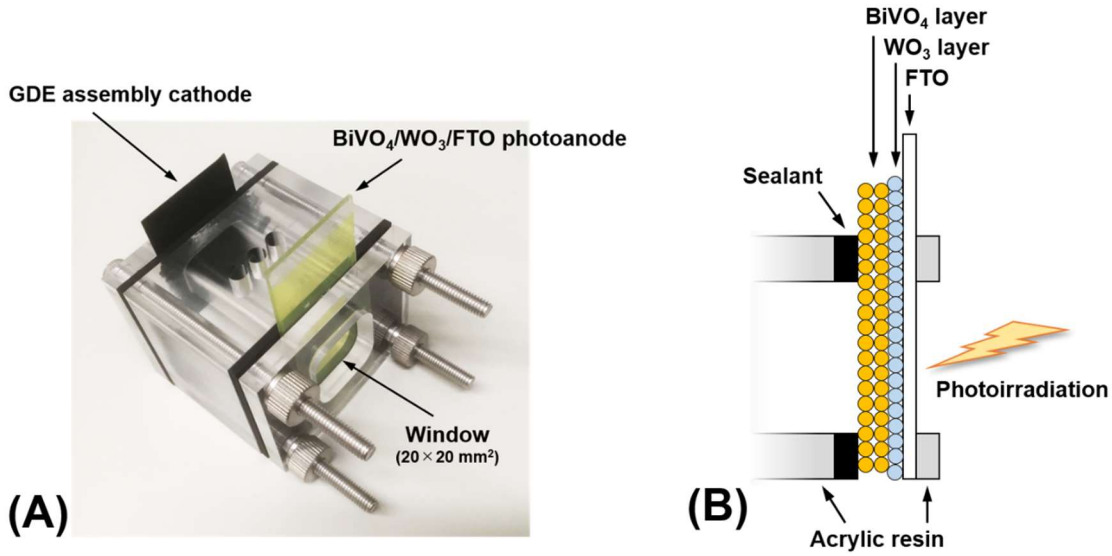

Figure S3 (A) Photograph of one-chamber electrolysis cell (made from acrylic resin). Both sides of the cell were sealed by a photoanode (yellow plate) and a cathode (black sheet) themselves, respectively. (B) Schematic illustration of the photoanode side. The simulated solar light irradiates the $BiVO_4/WO_3$/FTO photoanode from backside (FTO side) through the square window (4 cm^2).

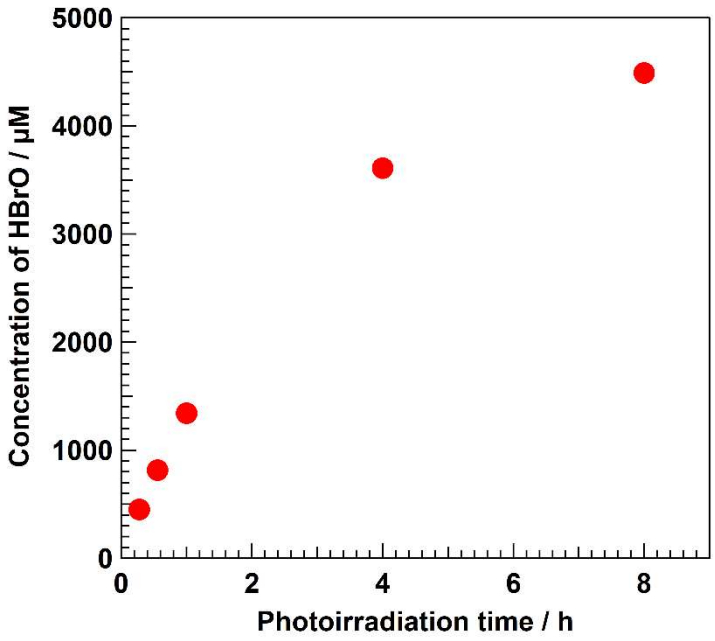

Figure S4 Time course of the HBrO concentration produced in the electrolyte solution ($\boldsymbol{C}_{\mathbf{HBrO}}$) during the photoelectrochemical reaction under solar light irradiation using 5.0 M NaBr as the electrolyte solution. Potentiostatic photoelectrolysis at +0.5 V vs. counter electrode. Light source: AM 1.5 simulated solar light. Anode: $BiVO_4/WO_3$/FTO 12 cm^2. Cathode: Pt wire (O_2 atmosphere). Volume of anolyte solution: 35 mL.

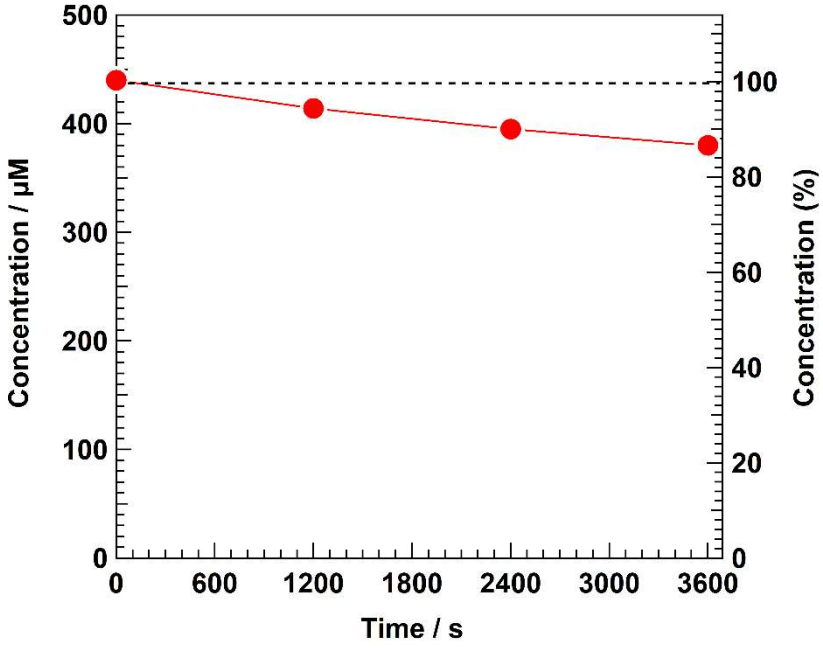

Figure S5 Time dependence of the HBrO concentration in 5.0 M NaBr aqueous solution under reaction conditions (with irradiation and slight stirring).

Table S2 Faradaic efficiency for HClO (***FE*$_{\mathbf{HClO}}$**) and HBrO (***FE*$_{\mathbf{HBrO}}$**) production in the photoelectrochemical oxidation of Cl^- and Br^- under solar light irradiation. Galvanostatic photoelectrolysis at 3.0 mA. Reaction time: 1000 s. Light source: AM 1.5 simulated solar light. Anode: $BiVO_4/WO_3$/FTO 12 cm^2. Cathode: Pt wire (O_2 atmosphere).

Electrolyte	FE_{HClO} (%)	Electrolyte	FE_{HBrO} (%)
Cl(200)ClO_4(300)	58	Br(200)ClO_4(300)	82
Cl(100)ClO_4(400)	41	Br(100)ClO_4(400)	82
Cl(10)ClO_4(490)	4.8	Br(10)ClO_4(490)	73

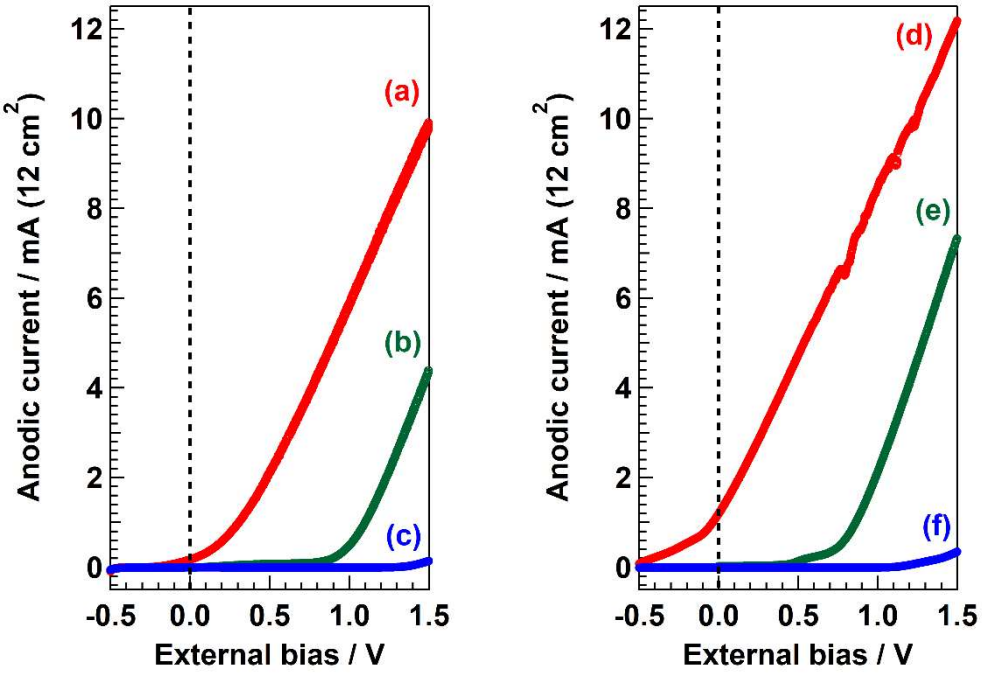

Figure S6 Photocurrent-external bias curves of the (a, d) $BiVO_4/WO_3$/FTO photoelectrode (12 cm^2), (b, e) Pt wire, and (c, f) FTO (12 cm^2) under solar light irradiation using (a, b, c) **Cl(50)ClO_4(450)** and (d, e, f) **Br(50)ClO_4(450)** as the electrolyte solution. Cathode: Pt wire (O_2 atmosphere).

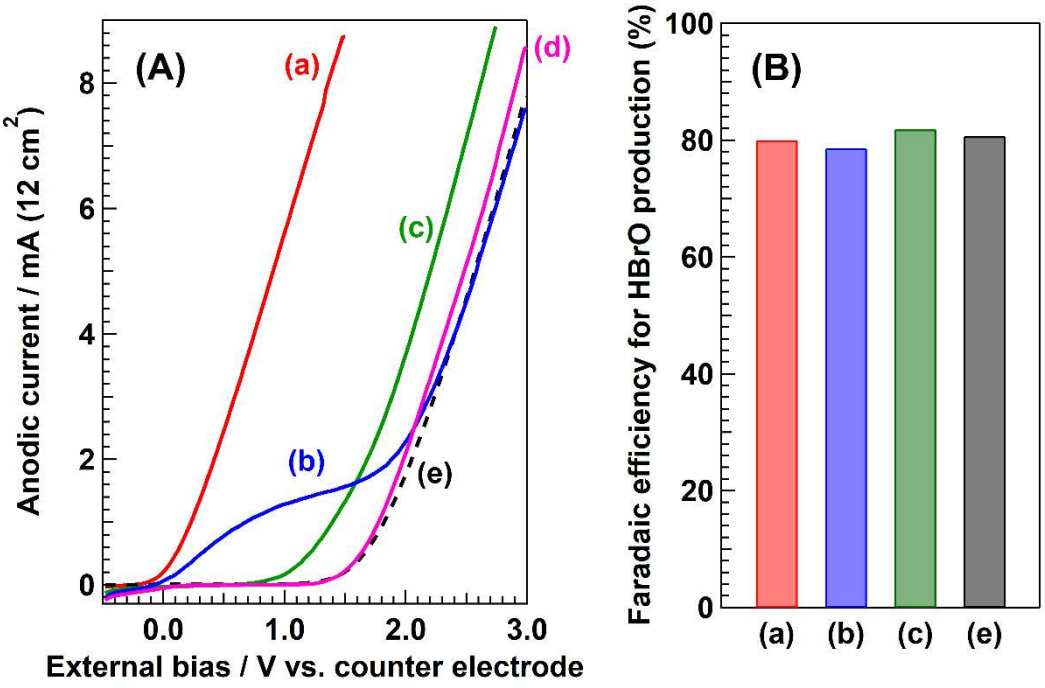

Figure S7 (A) Current-external bias curves in **Br(50)ClO$_4$(450)**, and **(B)** FE_{HBrO} in the galvanostatic photoelectrolysis at 3.0 mA for 1000 s using **Br(500)** electrolyte solution. (a) $BiVO_4/WO_3$/FTO, (b) WO_3/FTO, (c) $BiVO_4$/FTO, (d) FTO under solar light irradiation, and (e) $BiVO_4/WO_3$/FTO under dark condition. Anode: corresponding electrode 12 cm^2. Cathode: Pt wire (O_2 atmosphere).

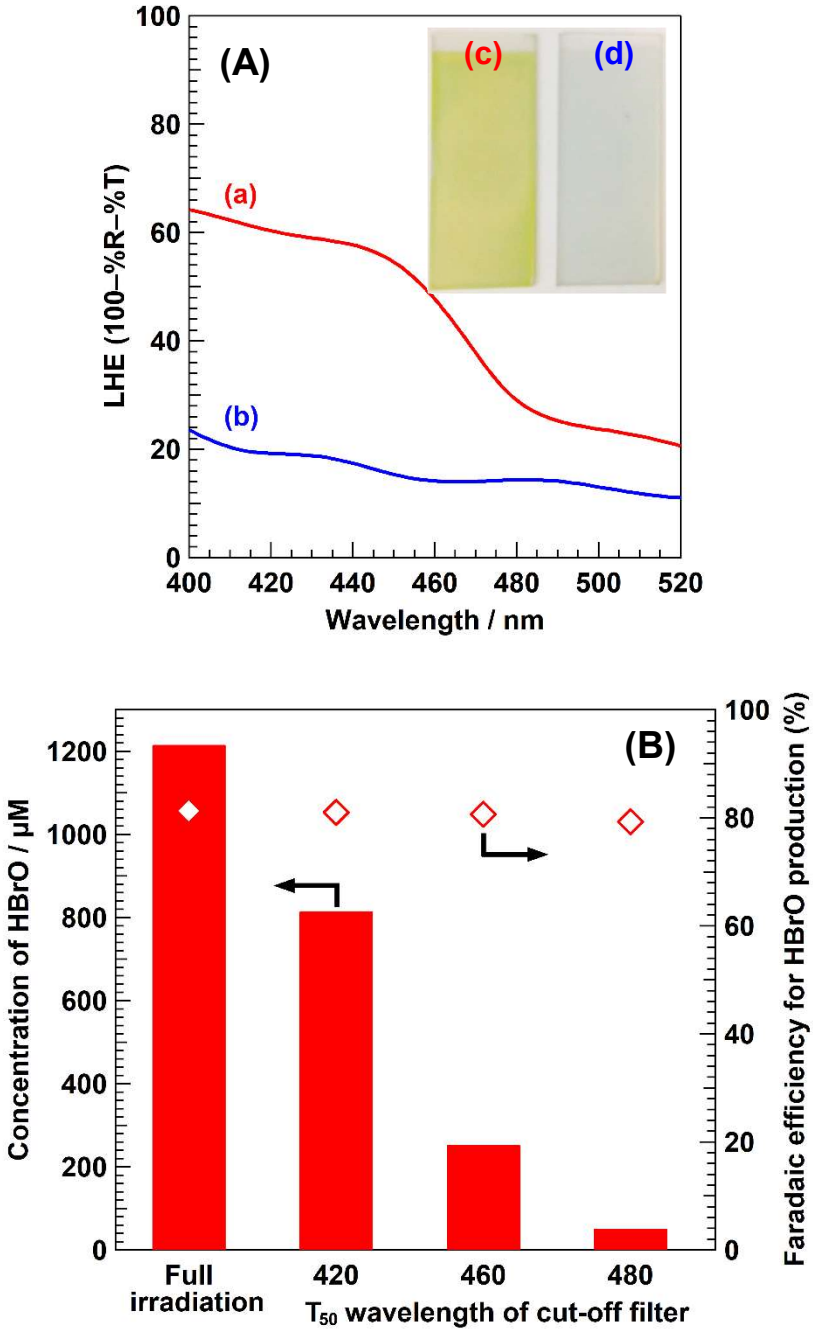

Figure S8 (A) Light harvesting efficiency (LHE) spectra of (a) $BiVO_4/WO_3$/FTO and (b) WO_3/FTO electrodes evaluated by transmittance (%T) and reflectance (%R), and photographs of (c) $BiVO_4/WO_3$/FTO and (d) WO_3/FTO electrodes. **(B)** C_{HBrO} and FE_{HBrO} in the potentiostatic photoelectrolysis using the $BiVO_4/WO_3$/FTO immersed in 5.0 M NaBr electrolyte solution under solar light irradiation with varied cut-off filter.

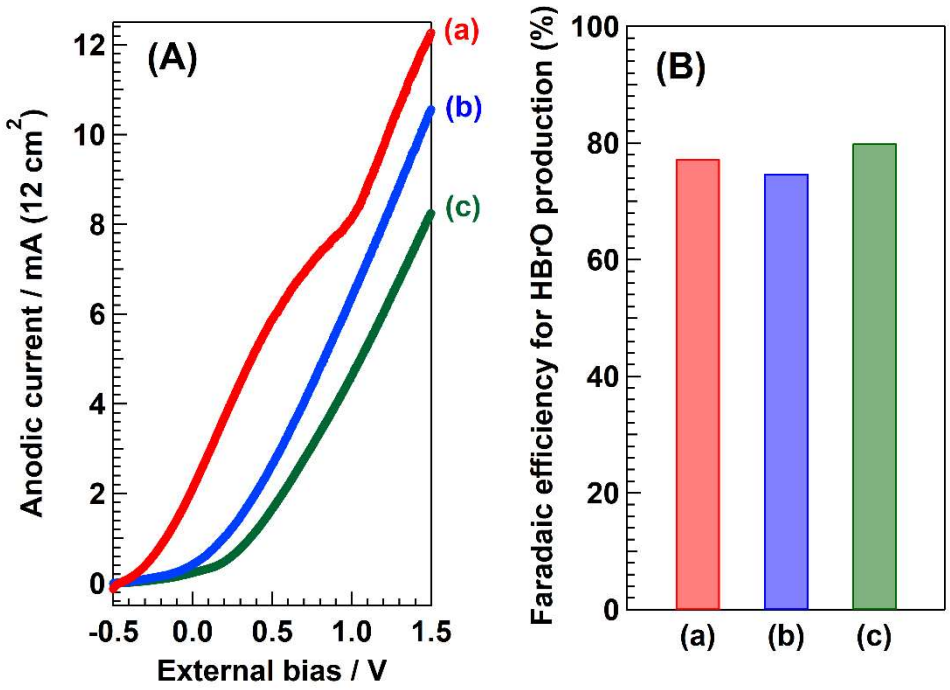

Figure S9 (A) Photocurrent-external bias curves of the $BiVO_4/WO_3$/FTO photoelectrode (12 cm^2) under solar light irradiation using **ClO_4(500)** as the electrolyte solution, and **(B)** FE_{HBrO} in the galvanostatic photoelectrolysis at 3.0 mA for 1000 s under solar light irradiation using **Br(500)** electrolyte solution. (a) undivided cell equipped with GDE cathode, (b) undivided cell using Pt wire cathode, and (c) divided cell with an ion exchange membrane using Pt wire cathode.

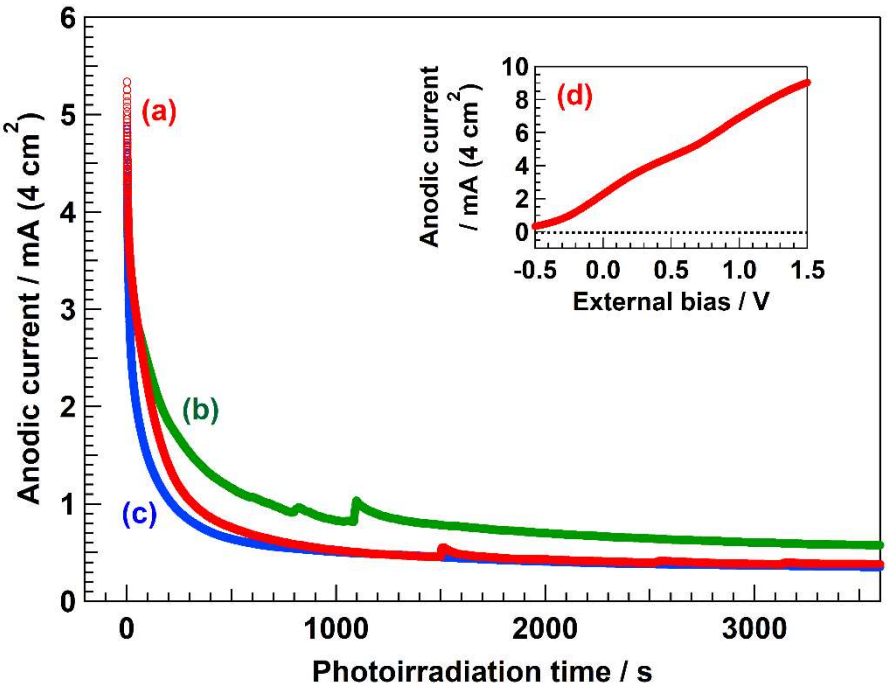

Figure S10 Time course of the anodic photocurrent the $BiVO_4/WO_3$/FTO photoelectrode (4 cm^2) under solar light irradiation in non-bias bleach production from (a) artificial sea water, (b) **Br(1)Cl(499)**, and (c) **Cl(500)** electrolyte solution. undivided cell equipped with Pt/C loaded GDE cathode (as shown in Figure S3) using 13 mL of electrolyte solution. (d) I-V curve measured before the reaction of (a).

It can be considered that there are two reasons for rapid decrease in the photocurrent. (1) insufficient gas diffusion in the cathode, and/or (2) poisoning of Pt cathode catalyst by chloride and bromide ions.